Unsupervised multispectral segmentation of SPOT images applied to nautical cartography.

J.-N. Provost[‡], C. Collet[‡], P. Pérez[•], P. Bouthemy [•]

[‡] Laboratoire GTS (Groupe de Traitement du Signal), Ecole Navale-French Naval Academy, BP 600, 29240 Brest-Naval France.

email: name@ecole-navale.fr

[•] IRISA/INRIA, Campus Universitaire de Beaulieu, 35042 Rennes cedex, France.

email: name@irisa.fr

Abstract

This paper presents an unsupervised image segmentation method based on Markov chains. It is applied to multispectral SPOT satellite images to recover nautical space charts. These images involve three spectral bands. The conditional distribution for each segmentation class is supposed to be Gaussian. The proposed method takes into account the correlation between the three spectral bands, and adresses the determination of the number of classes. Classification results on synthetic and real examples demonstrate the efficiency of the proposed method.

Keywords : *Markov chain, multispectral image segmentation, spectral correlation, estimation of parameters.*

1 Introduction

This paper is concerned with the segmentation of multispectral satellite images in an unsupervised way. Considered data are supplied by SPOT satellite which observes the earth in three spectral bands : XS1 channel covering 0.50 to 0.59 μm (green), XS2 channel covering 0.61 to 0.68 μm (red) and XS3 channel covering 0.79 to 0.89 μm (near infrared).

By combining these channels, colour composite images can be produced. In the sequel, the three considered channels will be denoted R,G,B standing for red, green and blue. Satellite sensors measure the radiometry, *i.e.*, the intensity of the radiations reflected by the ground or by the sea through the water layers. Spatial resolution is 20 by 20 meters.

Images we are interested in cover Pacific atolls. The goal of the segmentation step is to assign to each pixel a class label. In our application, these labels correspond to: cloud or cloud shadow, sea, ground. Then, in a future work, sea areas will have to be segmented according to the water depth, for production of nautical charts[6][9]. The motivation of directly exploiting these images is to reduce the cost in comparison with expensive hydrographic campaigns in Pacific Ocean. Furthermore, the accuracy and updating of nautical charts are especially important for navigation.

This paper is structured as follows. Section 2 describes the monospectral segmentation method based on Markov chains. Section 3 deals with the multispectral analysis. Results obtained on synthetic and real images are reported in section 4. Section 5 contains concluding.

2 Monospectral segmentation based on Markov chains

The interest of Markov chain methods[3][4] for image segmentation compared to 2D Markov field models[2][5][7] is that, being based on 1D modeling, they result in lower computing cost. To apply such a method, we need to transform a two dimensional set of pixels into a one dimensional set S. This transformation is realized by a Hilbert-Peano scan[8]. The performed segmentation then results in a 1D map, which is transformed into a 2D image using an inverse Hilbert-Peano scan.

2.1 Notations

We consider two sets of random variables: $X = (X_n)_{n \in S}$, the labels and $Y = (Y_n)_{n \in S}$, the observed data. X_n takes its value in a finite set of $\Omega = \{\omega_1, ..., \omega_K\}$ corresponding to K classes. n represents the position along the chain : $n = 1, ...; N$. We assume the noise in each spectral band to be Gaussian ($\mathcal{N}$). We suppose that the X is a first order Markov chain, i.e. :

$$P(X_{n+1}|X_n ... X_1) = P(X_{n+1}|X_n) \qquad (1)$$

We introduce the initial distributions $\pi_i = P[X_1 = \omega_i]$, and the transition matrix $a_{ij} = P[X_{n+1} = \omega_j | X_n = \omega_i]$.

At each iteration, we have to estimate simultaneously the initial distribution, the transition matrix and the Gaussian distributions $P(Y_s|X_s = \omega_i) = \mathcal{N}(\mu_i, \sigma_i)$.

We introduce the forward and backward probabilities :

$$\alpha_n(i) \quad = \quad P[X_n = \omega_i | Y_1 = y_1 ... Y_n = y_n] \qquad (2)$$

$$\beta_n(i) = \frac{P[Y_{n+1} = y_{n+1}...Y_N = y_N | X_n = \omega_i]}{P[Y_{n+1} = y_{n+1}...Y_N = y_N | Y_1 = y_1...Y_n = y_n]}$$

These probabilities can be calculated by backward and forward recursions[1]. We have the relation:

$$\begin{aligned} \xi_n(i) &= P[X_n = \omega_i | Y_1 = y_1...Y_N = y_N] \\ &= \alpha_n(i)\,\beta_n(i) \end{aligned} \quad (3)$$

We can find in the literature another definition of the backward and forward probabilites[1], but it suffers from underflow problem.

The *a posteriori* joint probability has also to be considered:

$$\Psi_n(i,j) = P[X_n = \omega_i, X_{n+1} = \omega_j | Y = y] \quad (4)$$

$$= \frac{\alpha_n(i) a_{ij} P(y_{n+1} | X_{n+1} = \omega_j)\,\beta_{n+1}(j)}{\sum_{l,m=1}^{K} \alpha_n(l) a_{lm} P(y_{n+1} | X_{n+1} = \omega_m)\,\beta_{n+1}(m)}$$

These probabilities allow us to update initial distributions, and transition matrix[4] using an EM procedure.

$$\pi_i^{[q+1]} = \xi_1^{[q]}(i) \quad (5)$$

$$a_{ij}^{[q+1]} = \frac{\sum_{n=1}^{N-1} \Psi_n^{[q]}(i,j)}{\sum_{n=1}^{N-1} \xi_n^{[q]}(i)} \quad (6)$$

Differents methods could be exploited to perform the segmentation step based on this modeling. We will describe our aproach.

2.2 Description of the algorithm

We use the ICE Gauss algorithm[4], based on Iterative Conditional Estimation. At the beginning, an estimation of the following parameters is required: $\Phi^{[0]} = \{\pi_i, a_{ij}, \mu_i, \sigma_i, (i,j) \in \{1,...,K\}\}$.

The different substeps of iteration $[q]$ are given below:

1. Compute $\alpha_n(i)$ and $\beta_n(i)$ using $\Phi^{[q-1]}$ parameter value.
2. Compute $\Psi_n(i,j)$ with equation (4).
3. Update a_{ij} and π_i using $\Psi_n(i,j)$ (equation (5)).
4. Generate x a realization of $X|Y = y$ using the *a posteriori* transition matrix (*cf* paragraph 2.3).
5. Update μ_i et σ_i with mean and variance estimators, applied on the area where $X_n = \omega_i$. We use $\delta(x_n, i) = 1$ if $x_n = \omega_i$, and 0 otherwise.
   - $\widehat{\mu_i} = \frac{\sum_{n=1}^{N} y_n \delta(x_n,i)}{\sum_{n=1}^{N} \delta(x_n,i)}$
   - $(\widehat{\sigma_i})^2 = \frac{\sum_{n=1}^{N} (y_n - \widehat{\mu_i})^2 \delta(x_n,i)}{\sum_{n=1}^{N} \delta(x_n,i)}$

After a predetermined number of iterations, the segmentation is performed by maximizing local *posterior* marginals (MPM estimation):

$$\begin{aligned} \hat{x}_n &= \arg \max_{i=1...K} P[X_n = \omega_i | Y_1 = y_1...Y_N = y_N] \\ &= \arg \max_{i=1...K} [\alpha_n(i)\,\beta_n(i)] \end{aligned} \quad (7)$$

2.3 Simulation of $X|Y = y$

In order to draw samples from $P(X|Y = y)$ in a recursive way, we rely on posterior transition probabilities

$$P[X_{n+1} | X_n, Y = y] \quad (8)$$

$$= P[X_{n+1} | X_n, Y_{n+1} = y_{n+1}, ..., Y_N = y_N]$$

$$P[X_1 = \omega_i | Y] = \frac{\pi_i P[Y_1 | X_1 = \omega_i]\,\beta_1(i)}{\sum_{l=1}^{K} \pi_l P[Y_1 | X_1 = \omega_l]\,\beta_1(l)} \quad (9)$$

$$P[X_{n+1} = \omega_j | X_n = \omega_i, Y_{n+1} = y_{n+1}, ..., Y_N = y_N]$$

$$= \frac{a_{ij} P[Y_{n+1} | X_{n+1} = \omega_j]\,\beta_{n+1}(j)}{\sum_{l=1}^{K} a_{il} P[Y_{n+1} | X_{n+1} = \omega_l]\,\beta_{n+1}(l)} \quad (10)$$

x_1 is drawn according to $P[X_1|Y]$, then x_{n+1} is drawn according to $P[X_{n+1}|X_n, Y_{n+1} = y_{n+1}, ..., Y_N = y_N]$ where x_n comes from previous sampling.

2.4 Number of classes

To perform an unsupervised segmentation, we need to determine the number of classes. We proposed to start with an upper bound for this number and to reduce it afterwards by merging classes whose distributions are too close.

We have considered the following criterion to merge classes i and j:

$$\left(\frac{\sigma_i + \sigma_j}{\sigma_i \sigma_j}\right) |\mu_j - \mu_i| < T \quad (11)$$

where μ_i and σ_i stand, respectively, for the mean and the standard deviation of class i. Threshold T is empirically set.

We have described the ICE Gauss algorithm in the monospectral case. Now, we introduce an extension of this method to multispectral images.

3 Multispectral segmentation based on Markov chains

The observed image is still represented by the random field $Y = (Y_n)$, but now $Y_n = (Y_n^{(R)}, Y_n^{(G)}, Y_n^{(B)})$, where R, G and B refer to the three channels available in SPOT

data. The new expression of the conditional law is given by :

$$P\left(Y_n = l | X_n = \omega_i\right) \tag{12}$$
$$= \frac{1}{(2\pi)^{3/2}} \frac{1}{\sqrt{\det\left(\Sigma_i\right)}} \exp\left[-\frac{1}{2}\left(l - M_i\right)^t \Sigma_i^{-1}\left(l - M_i\right)\right]$$

with M_i standing for the mean vector of class i and Σ_i representing the 3×3 covariance matrix:

$$M_i = \left[\begin{array}{ccc} \mu_i^{(R)} & \mu_i^{(G)} & \mu_i^{(B)} \end{array}\right]^t \tag{13}$$

$$\Sigma_i = \left[\begin{array}{ccc} {\sigma_i^{(R)}}^2 & \rho_i^{(RG)}\sigma_i^{(R)}\sigma_i^{(G)} & \rho_i^{(RB)}\sigma_i^{(R)}\sigma_i^{(B)} \\ \rho_i^{(RG)}\sigma_i^{(R)}\sigma_i^{(G)} & {\sigma_i^{(G)}}^2 & \rho_i^{(GB)}\sigma_i^{(G)}\sigma_i^{(B)} \\ \rho_i^{(RB)}\sigma_i^{(R)}\sigma_i^{(B)} & \rho_i^{(GB)}\sigma_i^{(G)}\sigma_i^{(B)} & {\sigma_i^{(B)}}^2 \end{array}\right]$$

One of the contributions of the proposed multispectral method resides in the fact that for each class, inter-channel correlations are estimated.

Thus, in the fifth step of the algorithm, the correlation coefficients are upded as follow:

$$\rho_i^{(C_1,C_2)} \tag{14}$$
$$= \frac{1}{\sqrt{\left[n_i \sum_{s\in S_i} y_s^{(C_1)2} - \left(\sum_{s\in S_i} y_s^{(C_1)}\right)^2\right]}} \times$$
$$\frac{n_i \sum_{s\in S_i} y_s^{(C_1)} y_s^{(C_2)} - \sum_{s\in S_i} y_s^{(C_1)} \sum_{s\in S_i} y_s^{(C_2)}}{\sqrt{\left[n_i \sum_{s\in S_i} y_s^{(C_2)2} - \left(\sum_{s\in S_i} y_s^{(C_2)}\right)^2\right]}}$$

where n_i is the number of pixels in class i, and S_i is the set of such pixels. (C_1, C_2) represents a pair of channels.

Moreover, in the fourth step of the algorithm, the label is selected in a probabilistic way with respect to the *a posteriori* transition matrix, using the tridimensional Gaussian law.

4 Results

4.1 Synthetic images

This unsupervised multispectral image segmentation has been first performed on synthetic images (Figure 1), where the ground truth is known), in order to validate the method.

The classification algorithm provides a perfect segmented map, and the estimation of parameters (including the correlation coefficients) is accurate (Table 1).

The size of the original image is 64 by 64 pixels. We start the algorithm with 10 classes, and the final result involing 5 classes is obtained after approximately 15 seconds of computing time (Workstation 43P IBM 120Mhz). Threshold T was set to 2.

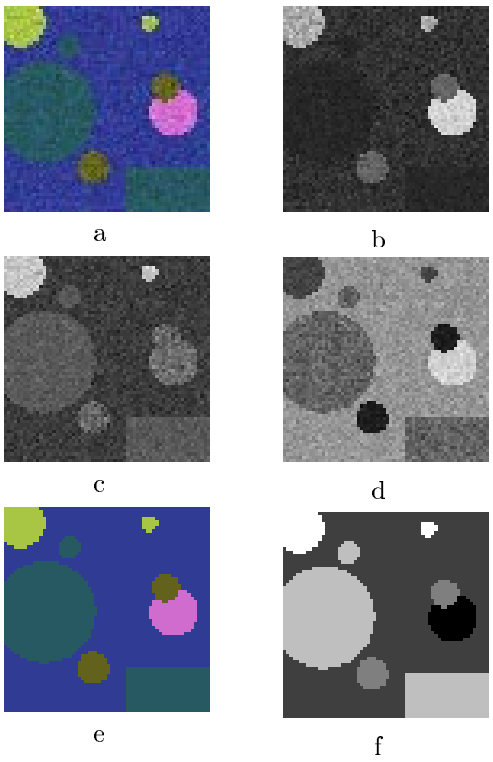

Figure 1: a) Original color image; b) Channel R of image 1a; c) Channel G of image 1a; d) Channel B of image 1a; e) Segmented image f) Ground truth

Parameters	Class 1	Class 2	Class 3	Class 4	Class 5
μ^R	210.4 210	49.9 50	100.1 100	40.0 40	169.8 170
μ^G	109.3 110	60.4 60	99.9 100	90.1 90	198.1 200
μ^B	208.6 210	149.3 150	29.1 30	99.2 100	68.5 70
σ^R	11.0 12	10.0 10	10.8 10	5.0 5	18.9 20
σ^G	16.4 18	11.1 11	19.2 20	9.0 9	14.0 15
σ^B	10.6 10	12.1 12	7.2 7	14.9 15	8.6 9
ρ^{RG}	0.31 0.4	0.22 0.2	-0.05 0	-0.16 -0.1	0.44 0.5
ρ^{RB}	-0.44 0.3	0.31 0.4	-0.60 -0.5	0.48 0.5	0.53 0.6
ρ^{GB}	0.12 0.2	0.80 0.8	0.66 0.7	0.68 0.7	0.66 0.7

Table 1: Estimated (first line) and true parameters (second line) of the synthetic image

In Figure 1, we can note that , if only one single band is considered, it is difficult to distinguish the five classes.

This demonstrates the interest of taking into account simultaneously the information from the three bands, which results in a perfect classification.

4.2 SPOT satellite images

We have applied our method to SPOT images, in the context of a nautical space chart application. The following experimental results (Figure 2) have been obtained with a multispectral SPOT image of 256 by 256 pixels. We can notice that in the original image (Figure 2a) waves disturb the radiometry. The initial number of classes was set to 8, and the final number is 6.

The multispectral algorithm allows us to exploit in an appropriate way the whole available information within the same segmentation process.

In the monospectral case, it is easy to initialize the conditional laws.We can, for example, choose for each class the standard deviation σ of the whole image. Then, we compute the mean μ of the whole image. The means of each class are:

$$\mu_i = \mu \pm k\frac{\sigma}{2} \; k = 1-\frac{K}{2},...,\frac{K}{2} \quad (k \text{ is supposed to be even})$$

In the multispectral case, we have to define three initial means for each class. In our method, they are chosen randomly, therefore the initial number of classes has to be high. The initial correlation coefficients are supposed to be equal to zero (i.e. the three Gaussian laws of a class are independent), and the initial values of standard deviations are still set great enough.

The drawback of a Markov chain model is to reduce the neighbourhood size of a pixel to two neighbours. Nevertheless, experimental results obtained prove that the tradeoff between speed and accuracy is better with this method (Table 1).

5 Conclusion

This paper has addressed the problem of unsupervised multispectral image segmentation using a Markov chain model. The results obtained both on synthetic and real images are quite promising.

This modeling approach based on 1D multispectral Markov chain leads to low computational time in comparison with usual methods based on 2D Markov fields requiring simulation by Gibbs sampler, and to an efficient solution for model parameters. The contributions of this work can be summarized as follows:

- we have introduce a mean to evaluate the number of classes. The *unsupervised* image segmentation only require an *a priori* upper bound for this number.
- the method is adapted to multisensor images. The proposed algorithm takes into account the correlation coefficients between the different channels within each class, which are estimated in an iterative way.

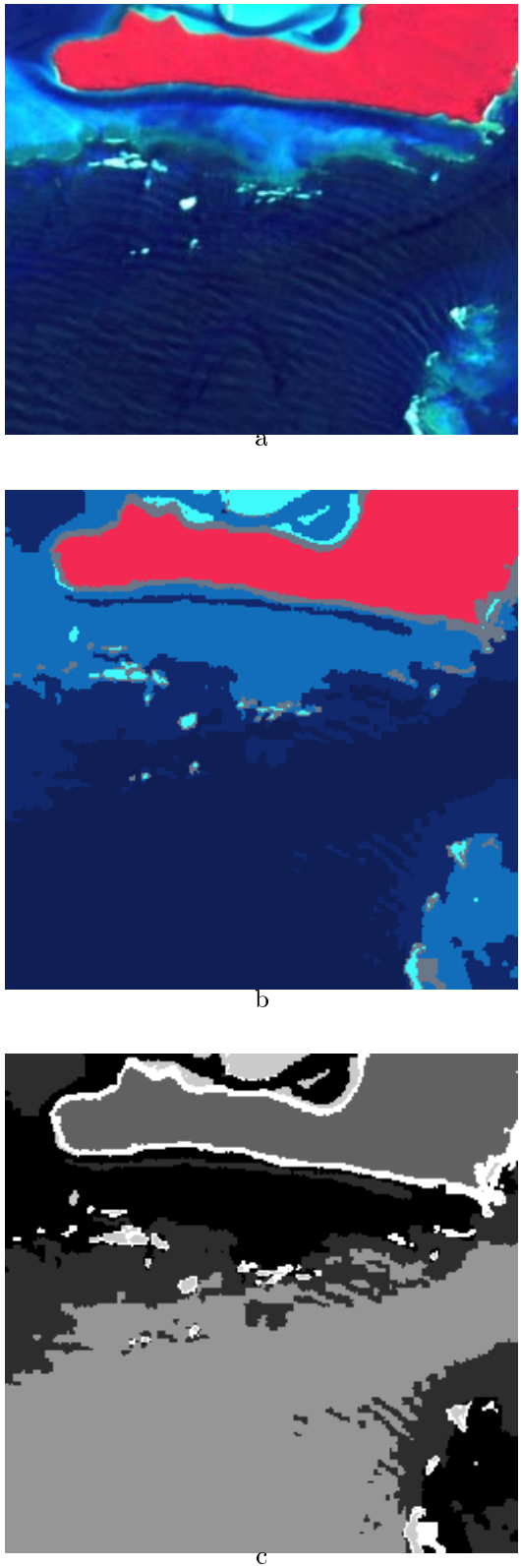

Figure 2: a) Original SPOT image b) Segmented image (color) c) Segmented image (grey level)

The accuracy of this method has been demonstrated on synthetic images (Figure 1 and Table 1), and convincing experiments on real images have been carried out (Figure 2).

References

[1] P. Devijver. Hidden Markov mesh random field models in image analysis. *Advances in Applied Statistics, Statistics and Images:1, Carfax Publishing Company*, pages 187–227, 1993.

[2] S. Geman and D. Geman. Stochastic relaxation, gibbs distributions and the bayesian restoration of images. *IEEE transactions on Pattern Analysis and Machine Intelligence*, 6:721–741, 1984.

[3] N. Giordana and W. Pieczynski. Unsupervised segmentation of multisensor images using generalized hidden Markov chains. *Proc. Int. Conf. on Image Processing (ICIP'96), Lausanne*, September 1996.

[4] N. Giordana and W. Pieczynski. Estimation of generalized multisensor hidden Markov chains and unsupervised image segmentation. *IEEE Transactions on Pattern Analysis and Machine Intelligence*, 19(5):465–475, 1997.

[5] J. Laferté, P. Pérez, and F. Heitz. Discrete Markov image modeling and inference on the quad-tree. *INRIA Research Report*, (1198), July 1998.

[6] L. Loubersac, P. Burban, O. Lemaire, H. Varet, and F. Chenon. Integrated study of Aitutaki's lagoon (cook islands) using Spot satellite data in situ measurements: bathymetric modelling. *Geocarto International (2)*, pages 31–37, 1991.

[7] M. Mignotte, C. Collet, P. Pérez, and P. Bouthemy. Unsupervised Hierarchical Markovian segmentation of sonar images. In *Proc. ICIP*, Santa Barbara, Califonie, USA, October 1997.

[8] J. Provine and R. Rangayyan. Lossless compression of Peano scanned images. *Journal of Electronic Imaging*, 3(2):176–181, 1994.

[9] S. Yu, M. Berthod, and G. Giraudon. Towards robust analysis of satellite images using map information - application to urban area detection. Technical Report 3293, INRIA, 1997.